Chemistry & Biology
Article

Designing Photoswitchable Peptides Using the AsLOV2 Domain

Oana I. Lungu,[1,2,3] Ryan A. Hallett,[1] Eun Jung Choi,[1] Mary J. Aiken,[1] Klaus M. Hahn,[2,3,*] and Brian Kuhlman[1,3,*]
[1]Department of Biochemistry and Biophysics
[2]Department of Pharmacology
[3]Lineberger Comprehensive Cancer Center
University of North Carolina, Chapel Hill, NC 27599, USA
*Correspondence: klaus_hahn@med.unc.edu (K.M.H.), bkuhlman@email.unc.edu (B.K.)
DOI 10.1016/j.chembiol.2012.02.006

SUMMARY

Photocontrol of functional peptides is a powerful tool for spatial and temporal control of cell signaling events. We show that the genetically encoded light-sensitive LOV2 domain of *Avena Sativa* phototropin 1 (AsLOV2) can be used to reversibly photomodulate the affinity of peptides for their binding partners. Sequence analysis and molecular modeling were used to embed two peptides into the Jα helix of the AsLOV2 domain while maintaining AsLOV2 structure in the dark but allowing for binding to effector proteins when the Jα helix unfolds in the light. Caged versions of the ipaA and SsrA peptides, LOV-ipaA and LOV-SsrA, bind their targets with 49- and 8-fold enhanced affinity in the light, respectively. These switches can be used as general tools for light-dependent colocalization, which we demonstrate with photo-activable gene transcription in yeast.

INTRODUCTION

Peptides regulate a variety of biological processes by acting as competitive inhibitors (Singh et al., 2005), allosteric regulators (Lockless and Ranganathan, 1999), and localization signals (Conti et al., 1998). Photocontrol of peptide activity is a powerful tool for precise spatial and temporal control of cellular function (Gautier et al., 2010; Nguyen et al., 2004). Typically, photo-activation of peptides has been achieved by covalently modifying peptides with chemical groups that inhibit function until they are removed by light (Möglich and Moffat, 2010; Young and Deiters, 2007). Because such derivatized peptides must usually be synthesized in vitro, one challenge of this approach is getting the peptides into living cells or animals. Additionally, in most cases the photo-induced reaction is not reversible. Recently, there has been considerable progress in the use of naturally occurring photo-activable proteins to engineer light switches that are genetically encoded and reversible (Kennedy et al., 2010; Levskaya et al., 2009; Wu et al., 2009; Yazawa et al., 2009). In the majority of cases, the goal has been to regulate the activity of folded protein domains. Here, we examine if the LOV2 domain from *Avena sativa* phototropin 1 (AsLOV2) can be used to photomodulate the affinity of peptides for binding partners (Huala et al., 1997).

AsLOV2 is part of the PAS superfamily of domains (Crosson and Moffat, 2001). It contains a flavin mononucleotide (FMN) cofactor located in the center of the PAS fold, as well as a large α-helical region C-terminal to the fold, termed the Jα helix (Halavaty and Moffat, 2007; Harper et al., 2003). Upon irradiation with blue light, a covalent adduct is formed between a cysteine side chain in the PAS fold and a carbon atom of the FMN (Crosson and Moffat, 2002; Swartz et al., 2001). Spectroscopy studies indicate that this leads to a large conformational change in the domain, including the unfolding of the Jα helix (Harper et al., 2004a; Swartz et al., 2002). When irradiation ceases, reversion of the thiol bond and conformational change back into the dark state occurs spontaneously within seconds to hours, depending on the LOV domain ortholog (Zoltowski et al., 2009).

The large conformation change that occurs within the Jα helix has been previously harnessed to create a photoswitchable GTPase termed PA-Rac (Wu et al., 2009); a photoswitchable variant of the *Escherichia coli* trp repressor that has enhanced affinity for DNA in the light termed LOV-TAP (Strickland et al., 2008, 2010); and a photo-activatable DHFR enzyme (Lee et al., 2008). In these studies, entire protein domains were fused to the end of the Jα helix in order to sterically occlude binding with effector molecules or perturb the conformational state of the attached domain. Upon blue light irradiation, unfolding of the Jα helix relieves the steric block or conformational strain.

Because peptides are more flexible than are folded domains, it may not be sufficient to place them at the end of the Jα helix to achieve a steric block; tighter caging may be obtained by embedding their functionality within the Jα helix (Figure 1). A similar strategy has been successful for caging coiled-coil peptides in the light-sensitive photo-active yellow protein (PYP; Fan et al., 2011). In the case of AsLOV2, the challenge is identifying sequences that incorporate the target binding of the peptide while maintaining the functionality of the Jα helix. One face of the Jα helix is exposed to solvent, while the other face forms hydrophobic interactions with a β sheet in the AsLOV2 domain. Residues on the surface of the helix are expected to be tolerant to mutation, whereas the buried residues should be more conserved. Similarly, most peptides have sets of residues that are required for binding target proteins, whereas other positions can be varied. These observations indicate that it may be possible to identify chimeric sequences for the Jα helix that maintain key interactions with the AsLOV2 domain but incorporate

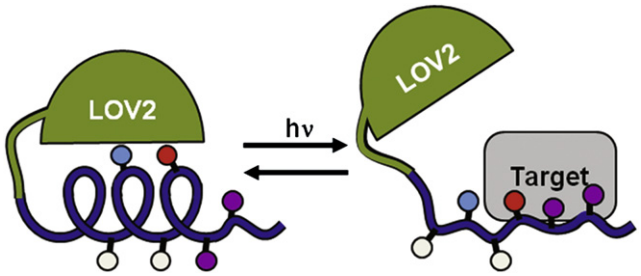

Figure 1. General Design Strategy for Caging Peptides Using the AsLOV2 Domain

Photoswitches are designed as sequence chimeras between the AsLOV2 Jα helix and the peptide to be caged. Residues that are important to AsLOV2-Jα interactions (cyan), important to peptide-target interaction (purple), important to both interactions (red), and residues that are important to neither interaction (white) are identified and mutated accordingly. Irradiation unfolds the Jα helix, and the peptide can bind its target.

residues critical to peptide function. In this study, we use sequence comparisons along with molecular modeling to create AsLOV2 variants that embed the binding properties of the ipaA (Tran Van Nhieu et al., 1997) and SsrA (Levchenko et al., 2003) peptides in the Jα helix.

The usefulness of a photoswitch depends on how much the activity is enhanced by light irradiation (dynamic range) as well as the absolute activity in the dark and in the light. Naturally occurring protein switches vary considerably with regard to absolute activities and dynamic range, indicating that the appropriate switching power for a particular application is likely to be system dependent. For instance, the AsLOV2-derived PA-Rac switch binds to its effector with an affinity of 2 μM in the dark and 200 nM in the light (Wu et al., 2009), which is appropriate for modulating cellular signaling because a similar change in binding affinity occurs when Rac1 naturally cycles between the GDP and GTP bound state (Thompson et al., 1998). Studies with the wild-type AsLOV2 domain indicate that it should be possible to create AsLOV2-based switches that show larger changes in activity upon light activation. Nuclear magnetic resonance (NMR) studies have shown that light activation changes the ratio of docked to undocked Jα helix from 98.4:1.6 in the dark to 9:91 in the lit state (Yao et al., 2008). This corresponds to a 3.8 kcal mol^{-1} change in free energy, which if efficiently harnessed could be used to create switches that have greater than 100-fold changes in binding affinity for target molecules. In scenarios that involve competitive binding to the Jα helix, that is, the helix is either docked against the LOV domain or bound to an effector molecule, it may be necessary to stabilize the helix docked state in order to take full advantage of the free energy perturbation that light activation provides. Strickland et al. (2010) showed that mutations that stabilize the docked Jα helix could be used to lower the dark state affinity of LOV-TAP for DNA and improve its dynamic range from 5- to 70-fold. Here, we identify further mutations that stabilize a docked Jα helix and show that the peptide switches can also be tuned by varying the location in which the caged sequence is embedded in the Jα helix and by varying the intrinsic affinity of the peptide for its target.

As an application of our tunable peptide photoswitches, we show that the caged ipaA peptide can be used to induce gene expression through light-activated heterodimerization in yeast, demonstrating that the caged peptides can be used as general tools for colocalizing proteins in living cells.

RESULTS

Identifying Peptides Compatible with AsLOV2 Caging

To identify protein binding peptides well suited for caging with the AsLOV2 domain, we searched the protein database (PDB) for peptide sequences similar to portions of the Jα helix. The similarity score for each position in the alignment was weighted based on how likely a match or mismatch was to disrupt caging or peptide binding. For instance, if a position in the alignment mapped to residues important for both the AsLOV2-Jα helix interaction and the peptide-protein interaction, then a large favorable score was given if the amino acids were identical, and a large unfavorable score was given if the amino acids were dissimilar. The importance of a residue to the AsLOV2-Jα helix interaction or the peptide-protein interaction was assigned based on how buried the residue was; residues that were more buried were considered more important. There was little reward or penalty for conserving amino acids on the surface of the Jα helix. Using a sliding window of six residues, the sequence of the Jα helix was aligned with over 3,000 peptide sequences taken from crystal structures of peptides cocrystallized with their protein binding partners. Peptides from several hundred structures were identified as candidates for caging with the AsLOV2 domain. It is worth noting that this approach can be expanded to also consider known protein binding peptides that have not been crystallized with their binding partners.

We picked out two peptide sequences for experimental testing and optimization: a vinculin binding peptide from the invasin protein ipaA (Izard et al., 2006) and the SsrA peptide from *E. coli,* which binds the protease delivery protein SspB (Levchenko et al., 2003). These sequences were chosen for a variety of reasons. First, at functionally important residues they align well with the Jα helix (Figures 2A and 2B). Indeed, several alternative alignments were identified for the SsrA peptide. Second, they adopt alternative conformations when binding their targets, ipaA adopts a helix, whereas SsrA binds in an extended conformation (Figure S1 available online). By testing both peptides, we examine if our approach can be used to cage peptides regardless of the conformation they adopt when bound to their target protein. Third, the peptides have different intrinsic affinities for their target proteins. IpaA binds the D1 domain of vinculin very tightly, $K_d < 1$ nM, whereas SrrA binds SspB with an affinity of ~30 nM.

Finally, they have complementary advantages for use in controlling cell biology. The SsrA and SspB sequences are specific to bacteria, and therefore it is expected that they will not interact with other proteins and peptides in higher organisms. Fusing proteins of interest to a photo-activable SsrA and SspB should provide a general approach for light-induced heterodimerization, which can be used to localize proteins in the cell and activate cell-signaling pathways. Vinculin and ipaA-like peptides are found in mammals, and therefore caged ipaA should only be useful as a general tool for colocalization in orthogonal systems, such as yeast. However, caged ipaA may be useful for probing vinculin biology in mammalian cells.

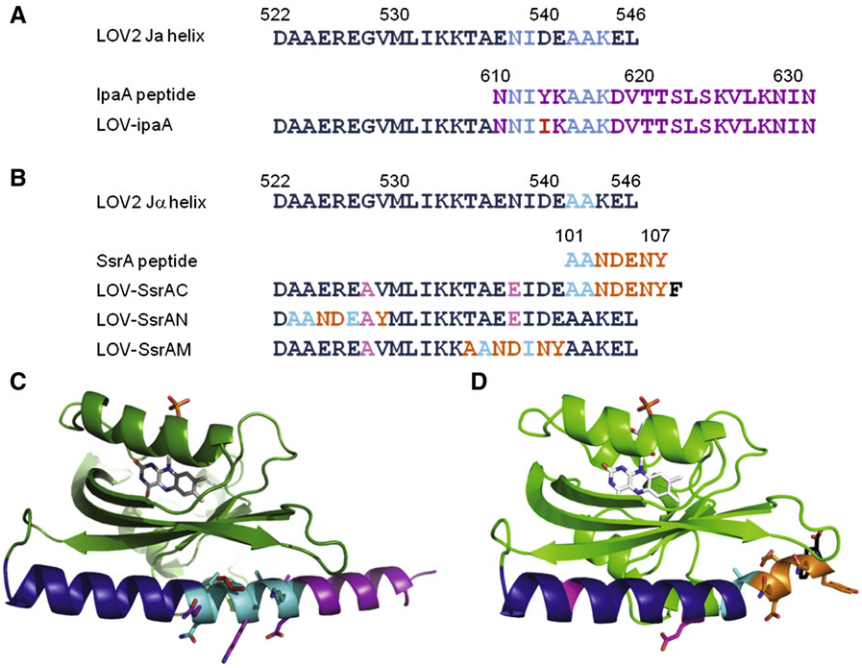

Figure 2. Design of LOV-ipaA and LOV-SsrA Peptide Photoswitches

(A) Sequence alignment of AsLOV2-Jα, ipaA, and LOV-ipaA. Jα sequence (blue), ipaA sequence (purple), chimera sequence (cyan), and designed residues (red) are indicated.

(B) Sequence alignment of AsLOV2-Jα helix, SsrA peptide, and three LOV-SsrA designs—LOV-SsrAC, LOV-SsrAN, and LOV-SsrAM. Jα helix sequence (blue), SsrA sequence (orange), chimera sequence (cyan), designed positions (black), and helix-stabilizing mutations (pink) are indicated.

(C) Model of LOV-ipaA with residues colored as in (A). Residues N538, I539, A542, and A543 K544 (cyan) as well as residues N537, K541, D545, V546 (purple), and I540 (red) are shown as sticks.

(D) Model of LOV-SsrAC with residues colored as in (B). Residues A528 and E538 (pink) as well as residues A542 and A543 (cyan) and N544, D545, E546, N547, and Y548 (orange) are shown as sticks.

See also Figure S1.

Vinculin is a protein that connects integrin binding proteins, such as talin (Cohen et al., 2006), to the actin cytoskeleton at focal adhesions (Saunders et al., 2006) and adherens junctions (Carisey and Ballestrem, 2011), cellular structures important for determining cell shape and motility. The ipaA peptide is from the IpaA protein of the *Shigella flexneri* bacterium and binds to the talin binding site on vinculin (Izard et al., 2006). It has been proposed that IpaA binding prevents vinculin from binding talin, and thus linking integrin signaling to the actin cytoskeleton. Selectively photo-controlling the binding of ipaA to vinculin through the LOV-ipaA photoswitch could render it useful as a dominant negative inhibitor of vinculin in mammalian cells and an integral tool for studying the role of vinculin dynamics in cell motility.

Design of LOV-ipaA

In our search of peptides in the protein database, the first ten residues of the ipaA VBS1 helical peptide were identified as a close match to the last ten residues of the AsLOV2 Jα helix (Figure 2A). Five of the ten positions are identical, and the hydrophobic residues on the Jα helix that make critical contacts with the AsLOV2 domain β sheet at residues 539, 542, and 543 are conserved in the alignment with ipaA. Additionally, residues in the ipaA sequence that make extensive contacts with vinculin are conserved in the alignment (Ile 612, Ala 615, Ala 616, and Val 619 in ipaA). This analysis suggests that it should be possible to design a chimeric sequence for the Jα helix that is compatible with the AsLOV2 structure and will bind vinculin when undocked from the AsLOV2 structure.

To design the chimeric sequence, the Rosetta molecular modeling program was used to assess the impact of altering the AsLOV2-Jα and vinculin-ipaA complex sequences (Das and Baker, 2008). Side-chain optimization simulations were used to thread the first ten residues of ipaA onto the last ten residues of the Jα helix. The Rosetta scores of individual residues were examined to determine if particular residues in the ipaA sequence packed unfavorably against the AsLOV2 domain β sheet. Only the mutation of the residue in position 540 from aspartic acid to tyrosine showed unfavorable scores. To search for an alternative amino acid to place at this position, Rosetta was used to perform a sequence optimization simulation in which position 540 was allowed to adopt alternative identities and neighboring side chains were free to adopt new side-chain conformations. One of the best scoring residues in the 540 position on the Jα helix was isoleucine. A working model for LOV-ipaA was then created by using the threaded AsLOV2-Jα design and adding the remaining eleven residues of ipaA onto the C-terminal end of Jα using the fragment insertion capability of Rosetta's domain assembly protocol (Figure 2C).

Dark- and Lit-State Binding between LOV-ipaA and Vinculin D1

We developed a fluorescence polarization competition assay to measure the binding affinity and kinetics of LOV-ipaA to the vinculin D1 subdomain under dark, as well as blue light, irradiation conditions (Figure 3A). LOV-ipaA was titrated into a mixture of the vinculin D1 subdomain bound to ipaA peptide labeled with the dye 5-(and-6)-Carboxytetramethylrhodamine (TAMRA). As LOV-ipaA bound to vinculin the dye-labeled peptide was competed off and its fluorescence polarization signal decreased. Initial experiments showed that the slow intrinsic off-rate of the ipaA peptide and LOV-ipaA from vinculin made it possible to monitor both the kinetics and thermodynamics of binding over a time course of several hours. Experiments with varying amounts of LOV-ipaA were fit simultaneously for the on rate and binding affinity of LOV-ipaA to vinculin D1 in Matlab using a numerical integration protocol.

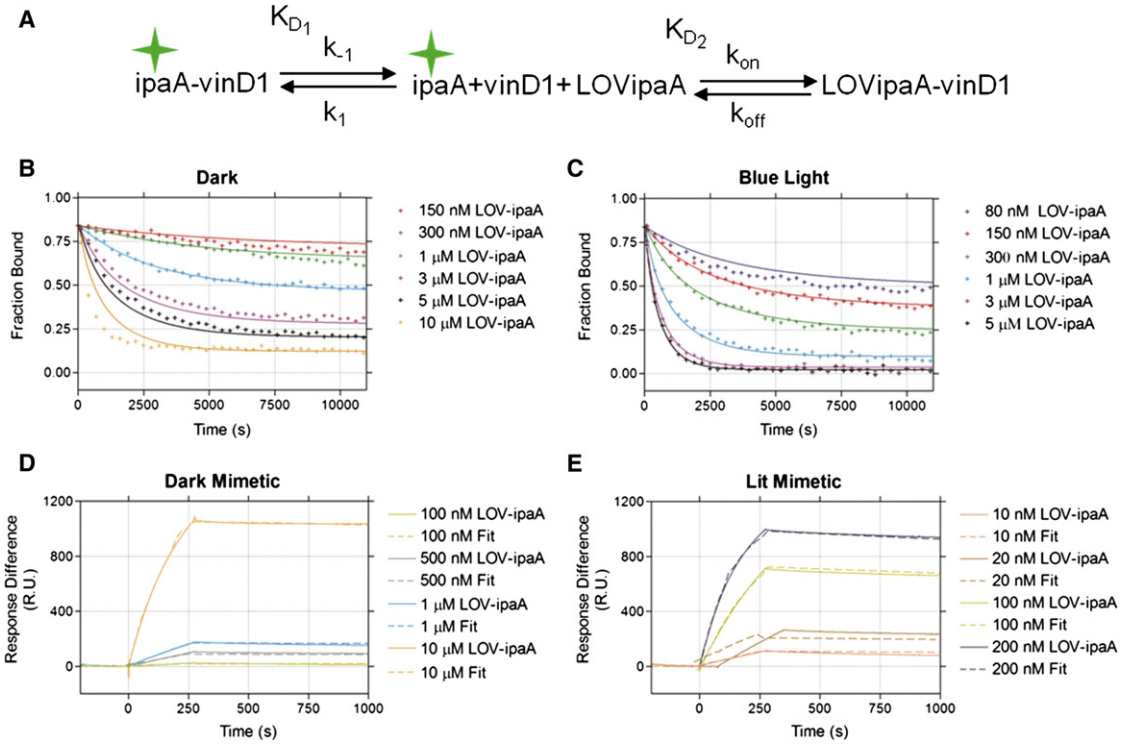

Figure 3. Measurement of Rates and Affinities of LOV-ipaA Binding to Vinculin

(A) Schematic of fluorescence polarization competition assay is shown. TAMRA-labeled ipaA (ipaA*) is bound to vinculin D1 subdomain (vinD1). Vinculin dissociates from the complex with rates k_{-1} and k_1 and binding affinity K_{D1}. LOV-ipaA (LOVipaA) binds vinculin with rates k_{on} and k_{off} and affinity K_{D2}. Fluorescence polarization decreases as the fraction of TAMRA-ipaA bound to vinculin decreases.

(B and C) Fraction of TAMRA-ipaA bound to vinculin over time with varying concentrations of LOV-ipaA titrated in the dark and (C) under blue light.

(D and E) Surface plasmon resonance measurements and first-order binding fit of LOV-ipaA L514K L531E C450A pseudodark and (E) LOV-ipaA L514K L531E I532E A536E pseudolit mutants.

See also Figure S2.

The same concentrations of LOV-ipaA under either blue light irradiation or dark-state conditions yielded different kinetic curves (Figures 3B and 3C). The binding affinity of LOV-ipaA WT in the light is 3.5 nM, whereas it is 69 nM in the dark, a 19-fold change (Table 1). The change in binding affinity upon light activation is primarily due to changes in the on rate for binding; in the dark, the rate constant is 1.3 × 10^3 M^{-1} s^{-1}, and in the light it is 1.4 × 10^4 M^{-1} s^{-1}. Similar changes were observed for LOV-ipaA mutants that abolish FMN-thiol bond formation (C450A) and lead to a pseudodark state or mutants that destabilized the Jα helix (I532E A536E), causing a pseudo-lit-state conformation. These results are consistent with the proposed mechanism of caging. In the dark, the Jα helix is primarily docked against the AsLOV2 domain, and the peptide is presented less frequently to the target binding site, slowing the on rate for binding. In general, the on rates for binding are slow both in the lit and dark state. Peptides and proteins often have k_{on} values greater than 1 × 10^5 M^{-1} s^{-1} (Alsallaq and Zhou, 2008). The slow rates observed here are consistent with the helix addition mechanism of ipaA binding to vinculin, wherein the vinculin D1 4-helix bundle is rearranged into a 5-helix bundle through the addition of ipaA (Nhieu and Izard, 2007).

Optimization of LOV-ipaA

We tested two sets of mutations predicted to enhance the dynamic range of the LOV-ipaA photoswitch. The first set of mutations was designed by Strickland et al. (2010) to stabilize the helical structure of Jα. The mutations, G528A and N538E, increased the dynamic range of the LOV-TAP photoswitch for its effector from 5- to 70-fold. When used in the LOV-ipaA system, the mutations did have a large effect on LOV-ipaA dark-state binding to vinculin D1, decreasing affinity more than 7-fold to 475 nM (Table 1). However, the mutations also weakened lit-state binding affinity over 10-fold to 110 nM. The net effect of the G528A and N538E mutations in LOV-ipaA then was a decrease in the photoswitching dynamic range of the protein. The weakened affinity for vinculin in the lit state is likely due to charge-charge repulsion between Glu538 in LOV-ipaA (G528A and N538E) and a glutamate close to the binding site of ipaA in vinculin.

We designed a second set of mutations to increase the dynamic range of the switch, L514K L531E, using the interactive modeling program FoldIt (Cooper et al., 2010). These mutations replaced two hydrophobic residues, one in the Jα helix, and the other on the β sheet contacting the Jα helix, with a salt bridge. The design was meant to stabilize interactions between the

Table 1. Kinetic Rates of LOV-ipaA Binding Vinculin D1

LOV-ipaA Construct	k_{on} (M^{-1} s^{-1})	k_{off} (s^{-1})	K_D (nM)
Dark mimetic (C450A)	$1.3 \pm 0.3 \times 10^3$	$8.0 \pm 0.7 \times 10^{-5}$	64 ± 9.5
WT dark	$1.4 \pm 0.1 \times 10^3$	$9.6 \pm 0.1 \times 10^{-5}$	69 ± 0.5
Lit mimetic (I532E A536E)	$2.9 \pm 2.0 \times 10^4$	$8.5 \pm 0.3 \times 10^{-5}$	3.0 ± 1.0
WT blue light	$1.3 \pm 0.3 \times 10^4$	$4.5 \pm 1.2 \times 10^{-5}$	3.5 ± 0.5
L514K L531E dark	$4.5 \pm 1.5 \times 10^2$	$1.1 \pm 0.4 \times 10^{-4}$	245 ± 5.0
L514K L531E blue light	$2.5 \pm 0.1 \times 10^3$	$1.3 \pm 0.1 \times 10^{-5}$	5.0 ± 0.1
G528A N538E dark	$1.8 \pm 0.3 \times 10^2$	$8.2 \pm 0.2 \times 10^{-5}$	475 ± 75
G528A N538E blue light	$8.0 \pm 2.0 \times 10^2$	$1.2 \pm 0.1 \times 10^{-4}$	160 ± 40

β sheet and Jα helix and lead to a more tightly bound helix in the dark state. Indeed, the binding affinity of LOV-ipaA L514K L531E to vinculin D1 in the dark state weakened to 245 nM, whereas the lit-state affinity increased only slightly to 5 nM. This set of mutations make LOV-ipaA a photoswitch with a 49-fold difference between the lit- and dark-state effector binding affinities.

To independently validate results from the florescence polarization competition assay, surface plasmon resonance experiments were also conducted. The on rate, off rate, and binding affinity of vinculin D1 to LOV-ipaA L514K L531E were measured. LOV-ipaA L514K L531E pseudolit (I532E A536E; Harper et al., 2004b) and pseudodark (C450A; Salomon et al., 2000) states were used. Pseudo-dark-state LOV-ipaA L514K L531E (Figure 3D) was able to bind vinculin D1 with an on rate of 4.5×10^2 M^{-1} s^{-1} and an off rate of 2.9×10^{-5} s^{-1}. A binding affinity of 64 nM was calculated from the kinetic data. The on rate was identical to that measured for LOV-ipaA L514K L531E under dark-state conditions using the fluorescence polarization assay. The off rate varied slightly, leading to a 4-fold difference in binding affinity between the two measurements. In part, the discrepancy might be due to the fact that it is difficult to fit an off rate that is so slow. Measuring the LOV-ipaA L514K L531E pseudolit photoswitch binding to vinculin D1, an on rate of 3.8×10^4 M^{-1} s^{-1} and an off rate of 8.7×10^{-5} s^{-1} were obtained (Figure 3E). Fitting indicated that the binding affinity was 2.3 nM. These values are similar to the kinetic rates measured for the LOV-ipaA lit mimetic using the fluorescence polarization assay.

There is a 49-fold increase in binding affinity for vinculin when LOV-ipaA L514K L531E is activated with light but binding in the dark is still considerable (245 nM). For some applications, it may be useful to have a switch that has weaker binding affinity in the dark. To test if we could switch the range of affinities over which LOV-ipaA functions, we made a mutation to LOV-ipaA that was predicted to reduce affinity for vinculin but should have negligible effect on the interactions between the Jα helix and the LOV domain. This mutant, L623A, weakened the affinity of the LOV-ipaA lit-state mimetic for the vinculin D1 domain from 3 nM to 2.4 μM, whereas the dark-state mimetic had no detectable binding as monitored with isothermal titration calorimetry, suggesting that binding in the dark is weaker than 40 μM (Figure S2).

Design and Optimization of LOV-SsrA

We extended the design strategy used to cage ipaA in order to create a second photoswitchable peptide, LOV-SsrA. The SsrA peptide interacts with the protease delivery protein SspB from *E. coli* as a linear epitope using the seven residue sequence AANDENY (Levchenko et al., 2003). Three possible alignments between SsrA and the Jα helix were identified in our PDB-wide search, one toward the N-terminal side of the helix (LOV-SsrAN), one near the C-terminal end (LOV-SsrAC), and one in the middle of the helix (LOV-SsrAM; Figure 2B). We first tested the C-terminal alignment LOV-SsrAC.

In LOV-SsrAC, the two alanines from SsrA were aligned with A542 and A543 from the last helical turn of the Jα helix, and the final three residues of the Jα helix were replaced with residues from the SsrA binding sequence (Figure 2D). Except for the last leucine, all buried positions in the Jα helix are conserved with this alignment, which only embeds the peptide in a single helical turn of the Jα helix. In comparison, the ipaA peptide is embedded within two helical turns in LOV-ipaA. To measure the affinity of LOV-SsrA for SspB in the dark and light, a fluorescence polarization competition assay was performed with TAMRA-labeled SsrA peptide (Nikolovska-Coleska et al., 2004). Unlike ipaA, SsrA binds rapidly to SspB and only equilibrium populations could be measured. The initial LOV-SsrA design showed a 2-fold change in affinity of 31 nM to 57 nM when activated with light (Table S1). As lit-state binding was near-native in affinity for SspB, approaches to stabilize the Jα helix and therefore decrease dark-state affinity were explored. We tested mutations previously shown to stabilize the Jα helix, G528A and N538E, as well as extensions to the C terminus of LOV-SsrAC. G528A and N538E had the desired effect and lowered dark-state affinity to 570 nM with a 5-fold change upon light activation. Extensions of varying lengths were designed with Rosetta (Kleiger et al., 2009) with the goal of binding the surface of the AsLOV2 domain, thereby constraining SsrA to a single, nonbinding conformation. The target surface on AsLOV2 was a hydrophobic patch immediately adjacent to the C terminus of the Jα helix. Two extensions were experimentally tested, the addition of a single phenylalanine and the addition of the sequence GYGNL. The longer extension had no detectable effect, whereas the single phenylalanine increased the dynamic range of the switch to 8-fold (Figure 4A).

The LOV-SsrAN designs incorporating the N-terminal alignment of SsrA had similar dynamic ranges to their corresponding C-terminal alignments. However, all had drastically reduced affinity for SspB in both the lit and dark state (>10 μM). The initial N-terminally aligned designs showed an approximate 2-fold increase in affinity after exposure to blue light. The addition of the G528A and N538E mutations slightly weakened the lit-state affinity for SspB to 12.6 μM and the dark-state affinity to 49 μM (Figure 4B). Because of constraints imposed by the AsLOV2 domain, the SspB binding sequence used in LOV-SsrAN was AANDEAY instead of AANDENY as used in LOV-SsrAC. To determine if the sequence change was responsible for the lower dark- and lit-state affinities for SspB, a peptide with the same sequence as LOV-SsrAN was synthesized and binding to SspB

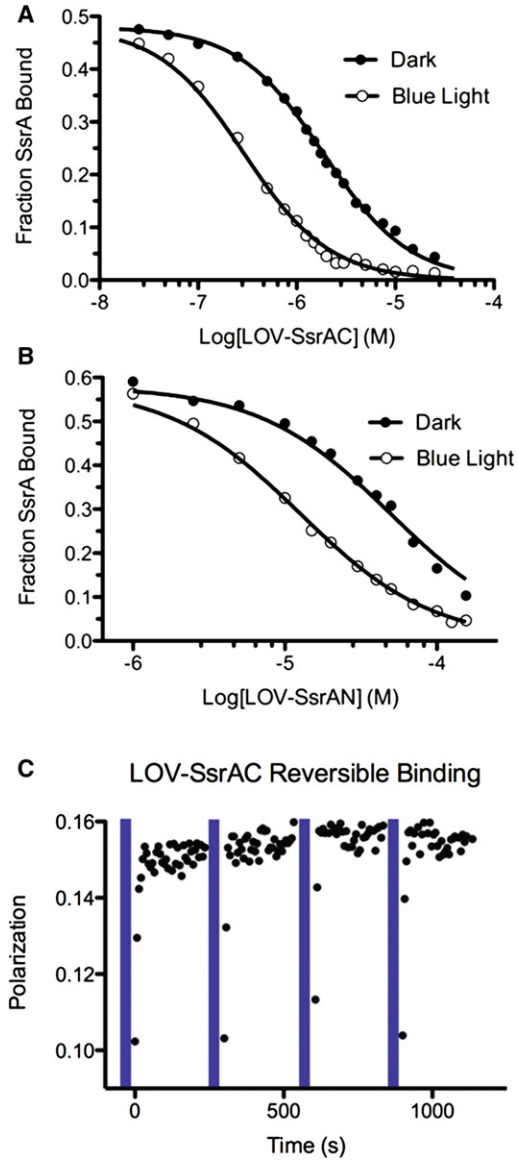

Figure 4. Competitve Binding of LOV-SsrA to SspB in Blue Light and in Darkness

(A and B) Competitive binding assay of LOV-SsrAC (A) or LOV-SsrAN (B) to an equilibrium solution of SspB and 5(6)TAMRA-SsrA. 5(6)TAMRA-SsrA becomes unbound as LOV-SsrA competes for SspB binding. Binding to SspB was measured immediately after illumination with blue light (open circles) and after return to dark state (closed circles).

(C) Reversible binding of LOV-SsrAC to SspB. A single titration point from the fluorescence polarization competition assay was repeatedly irradiated with blue light (blue bar = 60 s) and reversion to dark-state equilibrium was monitored by polarization.

See also Figure S3 and Table S1.

was measured. Binding was tight, 38 nM, suggesting that the reduced affinity for SspB was not because of changes to the binding sequence but rather because of the location within the Jα helix that the peptide was embedded. Results with LOV-SsrAM were more ambiguous, as the sequence embedded in the Jα helix, AANDINY, showed reduced affinity for SspB as a peptide (1.9 μM). However, lit- (40 μM) and dark-state (156 μM) state affinities were still significantly lower than that the isolated peptide, suggesting again that embedding sequences deeper in the Jα helix lowers accessibility to the peptide in both dark and light states (Figure S3).

The reversibility of LOV-SsrA switches was tested by monitoring their ability to compete with a TAMRA-labeled SsraA peptide for binding to SspB over multiple rounds of irradiation followed by incubation in the dark (Figure 4C). As monitored indirectly from following the fluorescence polarization signal from the SsraA peptide, the fraction of LOV-SsrA molecules switching from a bound to unbound state remained unchanged over multiple rounds of illumination, indicating that the switches are reversible. To check that the observed results were not an artifact due to interaction between the blue light and the TAMRA dye, similar reversion experiments were performed with only SspB and labeled peptide. No polarization changes were observed after incubation with blue light. The reversibility experiments also showed that dark-state equilibrium was reached within 15 s, quicker than what has been observed previously for the AsLOV2 domain. Half-times between 27 and 50 s have been reported for the LOV2 domain from *Avena sativa* (Salomon et al., 2000; Swartz et al., 2001). Using absorption spectroscopy, we determined the half-life of LOV-SsrAC's photocycle to be 2.7 ± 0.4 s, with a similar relaxation time in the presence of saturating concentrations of SspB(2.3 ± 0.1 s; Figure S3). At this point it is not clear why LOV-SsrAC has an unusually fast rate of reversion to the dark state, but this could be advantageous in applications in which quick switching from the bound to unbound state is critical.

LOV-ipaA Binding to Full-Length Vinculin: Actin Cosedimentation Assays

Having established that the AsLOV2 domain could be used to cage peptides, we tested if LOV-ipaA could be used to perturb vinculin in a biologically relevant manner. Actin cosedimentation assays were performed to measure the apparent binding affinity of LOV-ipaA to full-length vinculin. Vinculin naturally forms an autoinhibited conformation stabilized by interactions between the head (including the D1 domain) and tail domains. Binding of the ipaA peptide to the head domain competes with the autoinhibited state and releases the tail domain to bind with polymerized F-actin (Izard et al., 2006). Actin cosedimentation assays were performed to measure the apparent binding affinity of LOV-ipaA in the dark and lit state to full-length vinculin. In the assay, polymerized actin, vinculin, and LOV-ipaA (lit- or dark-state mutants) were incubated together (Figure 5A). Only vinculin that bound to LOV-ipaA should be able to interact and bind to F-actin. The resulting mix of bound and unbound vinculin was centrifuged at high speeds, resulting in fractionation of F-actin polymers out of solution, along with the vinculin-LOV-ipaA complexes that had bound to them. A sodium dodecyl sulfate polyacrylamide gel electrophoresis (SDS-PAGE) gel was used to monitor the amount of vinculin that fractionated out of solution along with F-actin as a function of the total concentration of vinculin, thereby determining the fraction of full-length vinculin bound to LOV-ipaA. The assay was repeated at several concentrations of LOV-ipaA to create a binding curve and calculate apparent binding affinities (Figures 5B and 5C). In general, the

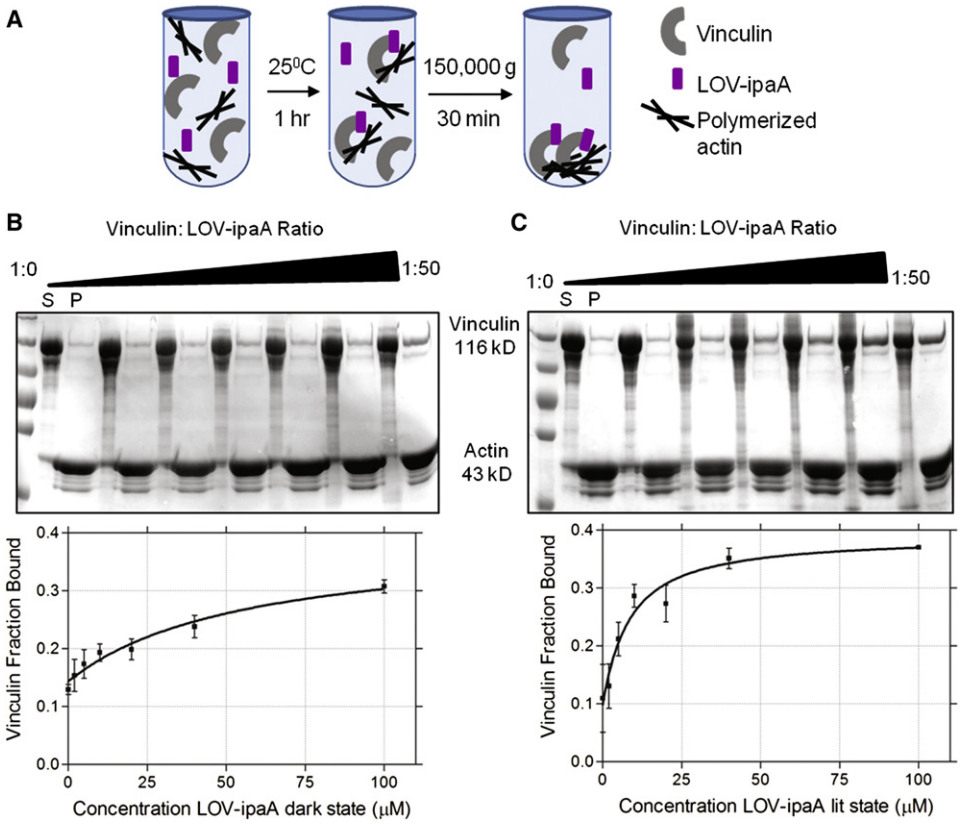

Figure 5. Binding of LOV-ipaA to Full-Length Vinculin Is Measured through an Actin Cosedimentation Assay

(A) Full-length vinculin, LOV-ipaA, and polymerized actin are incubated 1 hr at room temperature. Vinculin that is bound to LOV-ipaA will bind polymerized actin. The mixture is centrifuged at 150,000 g, pelleting polymerized actin and all vinculin bound to it out of solution.

(B and C) SDS-PAGE gel of LOV-ipaA C450A and (C) LOV-ipaA I532E A536E actin cosedimentation assay with vinculin. Molar ratios from 1:0 to 1:50 vinculin:LOV-ipaA were used. Supernatant (S) and pellet (P) fractions are shown side by side. Apparent binding affinity curves of fraction of vinculin bound to actin versus concentration of LOV-ipaA are plotted below. Error bars represent standard error of the mean.

See also Table S2.

affinities are expected to be considerably weaker with full-length vinculin than those observed for binding to the isolated D1 domain, because in the full-length protein there is competition with the autoinhibited state of vinculin (Le Clainche et al., 2010). For instance, peptides from the protein talin bind to the vinculin D1 domain with an affinity of 15 nM but bind to full-length vinculin with an affinity of ~5 μM (Izard and Vonrhein, 2004; Le Clainche et al., 2010). LOV-ipaA with the lit-state mutant bound with an apparent affinity of 8 μM to vinculin, whereas the dark-state mimetics bound with an affinity of 56 μM (Table S2). The binding of vinculin to ipaA in the presence of polymerized actin also gives us a window into the reactions that occur in vivo, where full-length vinculin must be bound both by talin and by F-actin in order to engage in integrin signaling. The difference in binding affinity between lit and dark states of LOV-ipaA to full-length vinculin in the presence of polymerized actin suggests that LOV-ipaA may be a relevant photoswitch for probing such signaling in vivo.

Photo-Activatable Yeast Transcription

To demonstrate that the caged peptides can be used to colocalize proteins and activate signaling events in living cells, we used the LOV-ipaA-vinculin D1 interaction as a heterodimerization switch for controlling gene expression. The experiments were performed in *Saccharomyces cerevisiae*, as it is an orthogonal system, lacking proteins that would cross-react with the LOV-ipaA-vinculin D1 interaction. We linked LOV-ipaA L623A to the GAL4 activation domain (AD), while linking vinculin D1 (vinD1) to the GAL4 binding domain (BD), and monitored the GAL4-induced activation of the transcriptional *GAL* promoter through a yeast two-hybrid assay. This is a strategy that has been widely used to identify protein-protein interactions. In our case, LOV-ipaA and vinculin D1 should only interact upon irradiation with blue light, thus bringing the GAL4 AD and BD into proximity (Figure 6A). The full GAL4 protein can then activate the expression of reporter genes downstream of the *GAL* promoter. We tested the ability to activate the reporter gene LacZ under both dark- and lit-state conditions through quantification of β-galactosidase activity (Figure 6B). We observed an activity of 5 Miller units under blue light conditions, 20 Miller units with the LOV-ipaA L623A lit-state mimetic, and 30 units using the ipaA peptide. Almost no activity (0.4 Miller units) was seen under dark or dark-state conditions, and no activity was seen in empty vector negative controls. We also tested activation of genes *MEL1*,

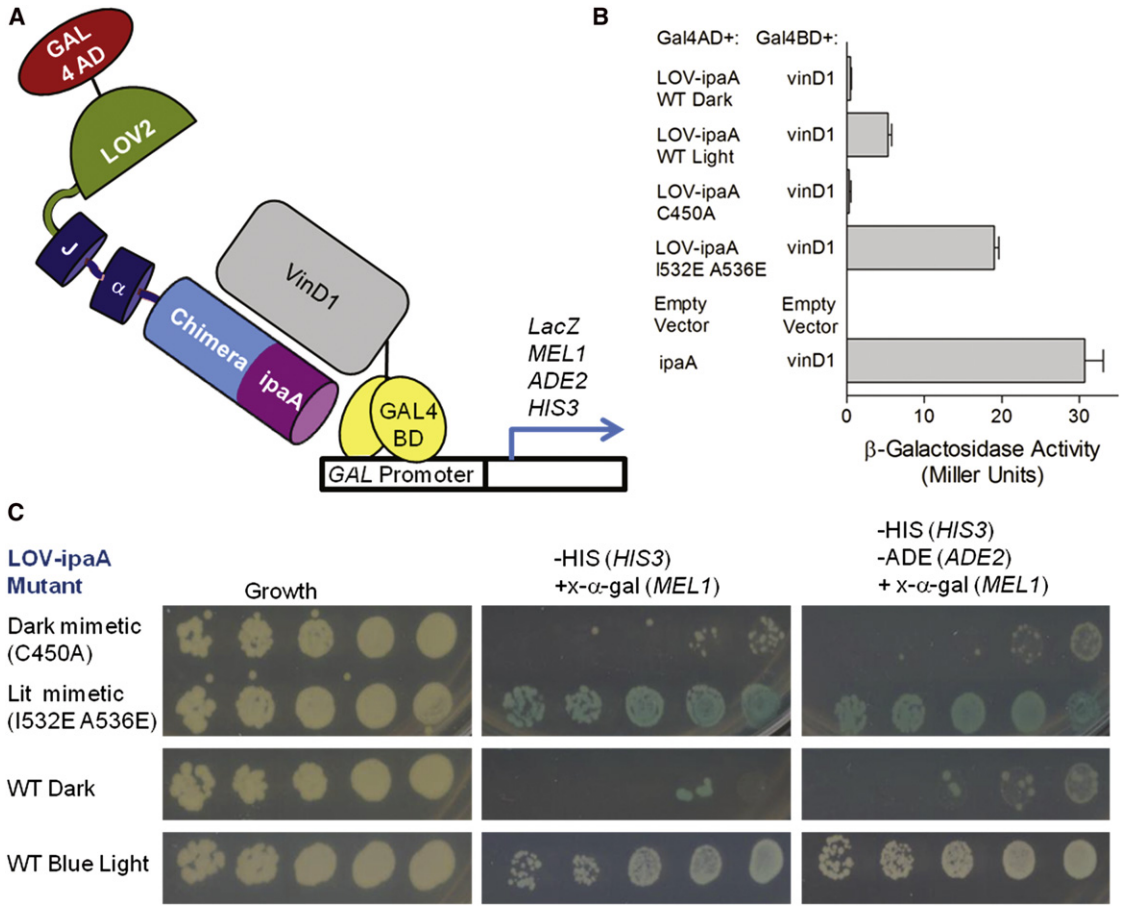

Figure 6. LOV-ipaA Is Used as a Light-Inducible Heterodimerization Tool

(A) LOV-ipaA L623A is linked to the GAL4 activation domain (AD), whereas vinculin D1 (vinD1) is linked to GAL4 binding domain (BD). Irradiation with blue light brings AD-LOV-ipaA into proximity to BD-vinD1, allowing for *GAL*-induced expression of reporter genes *LacZ*, *MEL1*, *HIS2*, and *ADE2*.

(B) LacZ expression is quantified. β-galactosidase activity of *S. cerevisiae*-mated strains containing BD and AD linked proteins, as specified, is shown. Error bars represent standard error of the mean.

(C) *S. cerevisiae*-mated strains containing BD-vinD1 and AD-LOV-ipaA mutants, as indicated, are grown in dark or blue light conditions on SD plates. Difference in levels of transcription of MEL1, HIS3, and ADE2 in dark- versus lit-state conditions is seen.

See also Figure S4.

HIS3, and *ADE2* under dark- and lit-state conditions by replica plating BD-vindD1 colonies mated with AD-LOV-ipaA L623A lit- and dark-state mimetic mutants or AD-LOV-ipaA L623A WT (Figure 6C). We saw strong growth of colonies containing LOV-ipaA L623A lit mimetic or WT grown in blue light on plates lacking His, as well as those lacking His and Ade, indicating expression of both *HIS3* and *ADE2* genes. Furthermore, colonies were blue, indicating expression of the *MEL1* gene, whose product, α-galactosidase, interacted with the x-α-gal substrate for blue screening. Colonies containing LOV-ipaA L623A dark mimetic or WT grown in the dark grew on control plates but did not grow on plates lacking His or Ade, showing low to no expression of *HIS2*, *ADE2*, or *MEL1* genes. This indicates that LOV-ipaA-vinculin D1 heterodimerization can be used as a tool to photocontrol yeast gene expression.

The LOV-ipaA L623A mutation was critical to achieving a lit- to dark-state change of phenotype in yeast gene expression. When experiments for *MEL1* and *HIS3* were conducted using LOV-ipaA lacking this mutation, no observable growth change was seen between colonies containing lit- and dark-state AD-LOV-ipaA mated with BD-vinD1 (Figure S4). The binding affinity of LOV-ipaA to vinculin D1 was hence so tight, even in the dark state, as to allow binding events and subsequent yeast gene expression to occur. The L623A mutation shifted the binding affinity of LOV-ipaA for vinculin D1 to a range in which there was no binding in the dark but significant activation in the light. This result highlights the usefulness of being able to tune the switches for specific applications.

DISCUSSION

We have shown that protein-binding peptides can be embedded in the AsLOV2-Jα helix so that their affinity for effector proteins is weakened in the dark but is enhanced when light-activation releases the Jα helix from the LOV domain. The approach is applicable to a variety of peptide sequences because only

a subset of residues on the Jα helix need to be conserved to maintain favorable interactions with LOV domain. Additionally, most protein-binding peptides contain residues that can be mutated without significantly weakening affinity for binding partners. In the case of LOV-ipaA and LOV-SsrAC, we also took advantage of the fact that not all of the peptide needs to be embedded in the Jα helix to create a steric block against effector binding. In this scenario, only a few residues from the N-terminal portion of the peptide need to be compatible with the folded Jα helix.

For some applications, it may be necessary to tune the designed photoswitch to have a dark-state activity and dynamic range compatible with the desired outcome. In the yeast two-hybrid experiments with LOV-IpaA, we found that we needed to weaken dark-state binding in order to prevent gene expression in the dark. We accomplished this by introducing a mutation that weakens the baseline affinity of IpaA for vinculin. Whereas the initial design switched from 3.5 nM to 69 nM affinity for vinculin, the mutant switched from 2.4 μM to >40 μM. The switching power of the LOV-peptide switches were also manipulated by introducing mutations that stabilize the interaction between the Jα helix and the rest of the LOV domain, as well as by varying how deeply the caged peptide was embedded in the helix. It was somewhat surprising that the SsrA peptide had significantly lower litstate affinity for SspB when embedded in the N-terminal portion of the Jα helix than when placed at the C terminus. NMR experiments with the WT AsLOV2 domain indicate that the helix undocks as a cooperative unit when the protein is activated with light (Yao et al., 2008). This suggests that there should be similar levels of access to residues in the N- and C-terminal regions of the Jα helix in the lit state; therefore, we expected that lit-state binding affinity for the peptide would be relatively insensitive to where the peptide was placed in the Jα helix. Our results indicate that the N-terminal portion of the Jα helix may be less accessible in the lit state, perhaps by transient interactions with the hydrophobic face of the LOV domain β sheet. Additionally or alternatively, the mutations we have made to the Jα helix to create LOV-SsrAN may have resulted in stronger interactions between the Jα helix and the rest of the AsLOV2 domain in the light.

Both the LOV-ipaA- vinculin D1 and the LOV-SsrA-SspB photo-activatable binding interactions can be harnessed as tools for photo-activatable heterodimerization. The LOV-ipaA-vinculin switch can be used in bacteria and in yeast cells, as these systems do not contain vinculin or vinculin binders that would affect the LOV-ipaA-vinculin interaction. On the other hand, the LOV-SsrA-SspB photo-activatable heterodimerization binders should be useful in higher organisms, such as mammalian cells. LOV-ipaA has a very slow off rate for vinculin D1, so it is better suited for long timescale applications, such as yeast mating. In contrast, LOV-SsrA binding to SspB is rapidly reversible so can be used for more transient interactions, such as single cell motility experiments. In these ways, both LOV-ipaA and LOV-SsrA should be useful tools to spatially and temporally bring together proteins for activating signaling cascades.

SIGNIFICANCE

Peptides regulate a variety of biological processes by acting as competitive inhibitors, allosteric regulators, and localization signals. Photocontrol of peptide activity is a powerful tool for precise spatial and temporal control of cellular function. Our work in this paper focuses on designing and characterizing peptides caged by embedding their sequences into the Jα helix of the AsLOV2 domain. The peptides ipaA and SsrA were both effectively caged in this manner, allowing for enhanced peptide-effector binding in the light. Mutations introduced into the AsLOV2 domain increased the difference between lit- and dark-state effector binding, whereas the position in which the caged sequence is embedded in the Jα helix and the intrinsic affinity of the peptide for its target tunes the range of affinities of the photoactivatable peptide. We discuss ways in which other peptides may be caged in a similar manner using the AsLOV2 domain. We also apply LOV-ipaA as a tool for photo-activatable gene expression in *Saccharomyces cerevisiae* and describe potential uses for LOV-SsrA.

EXPERIMENTAL PROCEDURES

Cloning

The LOV-ipaA gene was synthesized with a six histidine N-terminal tag (Genscript, Piscataway, NJ, USA) and cloned into the pET21b vector. The genes for LOV-SsrA and monomeric SspB were synthesized (Genscript) and cloned into pQE-80L and pTriEX4 vectors, respectively. All mutations were performed using site-directed mutagenesis. The vinculin D1 subdomain (residues 1–258) and full-length vinculin (residues 1–1066) were cloned into a pET15b vector. See Supplemental Experimental Procedures for protein expression and purification.

Peptides

Peptides containing the sequence TANNIIKAAKDATTSLSKVLKNIN, TANNII KAAKDATTSASKVLNIN, TANNIIKAAKDATTSLSKALKNIN, QIEEAANDENY, LIKKAANDINYAAK, and HVRDAANDEAYMLIK were synthesized at UNC-Chapel Hill and amine labeled using 5-(and-6)-Carboxytetramethylrhodamine (TAMRA) dye (Anaspec, Fremont, CA, USA). Peptide concentration was determined by measuring absorbance of the TAMRA dye at 555 nm using 65,000 M^{-1} cm^{-1} extinction coefficient.

Fluorescence Polarization Experiments

All fluorescence polarization experiments were conducted using a Jobin Yvon Horiba FluoroMax3 fluorescence spectrometer. TAMRA-labeled peptides were excited with polarized light at 555 nm, and the polarization of emitted light was measured at 583 nm. See Supplemental Experimental Procedures for detailed methods.

Surface Plasmon Resonance

Surface plasmon resonance experiments were conducted using a Biacore 2000 machine (GE Healthcare, Waukesha, WI, USA). Vinculin D1 was immobilized through amine coupling to the surface of a CM5 chip (GE Healthcare). Different concentrations of LOV-ipaA mutants were flown over the immobilized protein, and the change in response units over time was recorded. Data were fit simultaneously for k_{on} and k_{off} to a pseudo-first-order binding model.

Actin Cosedimentation Assays

Purified rabbit actin (Invitrogen) was polymerized for 30 min at room temperature in 10 mM Tris-HCl (pH 7.5) containing 100 mM KCl, 2 mM $MgCl_2$, 2 mM DTT, and 1 mM ATP. Vinculin (2 μM) and either ipaA peptide or LOV-ipaA mutants were mixed for vinculin:ipaA rations of 1:0, 1:1, 1:2.5, 1:5, 1:10, 1:20, or 1:50 per sample. Polymerized actin (12 μM) was added to each sample, within a volume of 45 μl per sample. Samples were incubated at room temperature for 1 hr. They were then centrifuged in a TLA-100 rotor in a Beckman Coulter Optimax XP ultracentrifuge at an acceleration of 150,000 g for 30 min cooled to 20°C. Samples were split into supernatant and pellet fractions. Pellets were resuspended into 45 μl 2x tris-glycine SDS

buffer. All fractions were denatured and run onto an 8% SDS-PAGE polyacrylamide gel. Gels were Coomassie stained and analyzed using ImageJ software to determine the fraction of vinculin present in the pellet versus total vinculin in each sample (Le Clainche et al., 2010).

Yeast Two-Hybrid Assays

LOV-ipaA L623A WT, lit-state mutants, dark-state mutants, and ipaA were cloned into a pGADT7 vector and transformed into *S. cerevisiae* Y187 strain, whereas the vinculin D1 subdomain was cloned into a pGBKT7 vector and transformed into *S. cerevisiae* Y2Hgold strain (Clontech, Mountain View, CA, USA). Empty vectors were also transformed into the appropriate strains. Transformed colonies of Y2Hgold and Y187 were mated at 30°C overnight and plated on synthetic dextrose (SD) –Leu –Trp media. For yeast two-hybrid experiments, mated colonies were serially diluted (1:5, from right to left on plates shown) and replica plated onto SD –Leu –Trp media; SD –Leu –Trp media with auerobasidin A and 5-bromo-4-chloro-3-indolyl-α-D-gactopyranoside (x-α-gal); SD –Leu –Trp –His media with auerobasidin A and x-α-gal; and SD –Leu –Trp –His –Ade media with auerobasidin A and x-α-gal. Plates were grown for three days at 30°C. For Miller assays, mated colonies were picked and grown to saturation in SD –Leu –Trp media. Saturated colonies were diluted to low-log phase and grown for 4 hr under dark or blue light conditions. Cells were lysed open and treated with chlorophenol red-β-D-galactopyranoside (CPRG; Roche) substrate to determine β-galactosidase activity in Miller units (Kennedy et al., 2010).

SUPPLEMENTAL INFORMATION

Supplemental Information includes four figures, two tables, and Supplemental Experimental Procedures and can be found with this article online at doi:10.1016/j.chembiol.2012.02.006.

ACKNOWLEDGMENTS

We thank A. Tripathy and the Macromoleular Interaction core facility at UNC-Chapel Hill for help in biophysical experiments, C. A. Purbeck for help and advice in conducting yeast 2-hybrid experiments, and M. Rougie for help with vinculin studies. This work was supported by grants from the National Institutes of Health (GM093208 and GM057464) and the American Heart Association (09PRE2100055 to O.I.L.).

Received: November 10, 2011
Revised: January 12, 2012
Accepted: February 1, 2012
Published: April 19, 2012

REFERENCES

Alsallaq, R., and Zhou, H.-X. (2008). Electrostatic rate enhancement and transient complex of protein-protein association. Proteins *71*, 320–335.

Carisey, A., and Ballestrem, C. (2011). Vinculin, an adapter protein in control of cell adhesion signalling. Eur. J. Cell Biol. *90*, 157–163.

Cohen, D.M., Kutscher, B., Chen, H., Murphy, D.B., and Craig, S.W. (2006). A conformational switch in vinculin drives formation and dynamics of a talin-vinculin complex at focal adhesions. J. Biol. Chem. *281*, 16006–16015.

Conti, E., Uy, M., Leighton, L., Blobel, G., and Kuriyan, J. (1998). Crystallographic analysis of the recognition of a nuclear localization signal by the nuclear import factor karyopherin α. Cell *94*, 193–204.

Cooper, S., Khatib, F., Treuille, A., Barbero, J., Lee, J., Beenen, M., Leaver-Fay, A., Baker, D., Popović, Z., and Players, F. (2010). Predicting protein structures with a multiplayer online game. Nature *466*, 756–760.

Crosson, S., and Moffat, K. (2001). Structure of a flavin-binding plant photoreceptor domain: insights into light-mediated signal transduction. Proc. Natl. Acad. Sci. USA *98*, 2995–3000.

Crosson, S., and Moffat, K. (2002). Photoexcited structure of a plant photoreceptor domain reveals a light-driven molecular switch. Plant Cell *14*, 1067–1075.

Das, R., and Baker, D. (2008). Macromolecular modeling with rosetta. Annu. Rev. Biochem. *77*, 363–382.

Fan, H.Y., Morgan, S.-A., Brechun, K.E., Chen, Y.-Y., Jaikaran, A.S.I., and Woolley, G.A. (2011). Improving a designed photocontrolled DNA-binding protein. Biochemistry *50*, 1226–1237.

Gautier, A., Nguyen, D.P., Lusic, H., An, W., Deiters, A., and Chin, J.W. (2010). Genetically encoded photocontrol of protein localization in mammalian cells. J. Am. Chem. Soc. *132*, 4086–4088.

Halavaty, A.S., and Moffat, K. (2007). N- and C-terminal flanking regions modulate light-induced signal transduction in the LOV2 domain of the blue light sensor phototropin 1 from Avena sativa. Biochemistry *46*, 14001–14009.

Harper, S.M., Neil, L.C., and Gardner, K.H. (2003). Structural basis of a phototropin light switch. Science *301*, 1541–1544.

Harper, S.M., Christie, J.M., and Gardner, K.H. (2004a). Disruption of the LOV-Jalpha helix interaction activates phototropin kinase activity. Biochemistry *43*, 16184–16192.

Harper, S.M., Neil, L.C., Day, I.J., Hore, P.J., and Gardner, K.H. (2004b). Conformational changes in a photosensory LOV domain monitored by time-resolved NMR spectroscopy. J. Am. Chem. Soc. *126*, 3390–3391.

Huala, E., Oeller, P.W., Liscum, E., Han, I.S., Larsen, E., and Briggs, W.R. (1997). Arabidopsis NPH1: a protein kinase with a putative redox-sensing domain. Science *278*, 2120–2123.

Izard, T., and Vonrhein, C. (2004). Structural basis for amplifying vinculin activation by talin. J. Biol. Chem. *279*, 27667–27678.

Izard, T., Tran Van Nhieu, G., and Bois, P.R. (2006). Shigella applies molecular mimicry to subvert vinculin and invade host cells. J. Cell Biol. *175*, 465–475.

Kennedy, M.J., Hughes, R.M., Peteya, L.A., Schwartz, J.W., Ehlers, M.D., and Tucker, C.L. (2010). Rapid blue-light-mediated induction of protein interactions in living cells. Nat. Methods *7*, 973–975.

Kleiger, G., Saha, A., Lewis, S., Kuhlman, B., and Deshaies, R.J. (2009). Rapid E2-E3 assembly and disassembly enable processive ubiquitylation of cullin-RING ubiquitin ligase substrates. Cell *139*, 957–968.

Le Clainche, C., Dwivedi, S.P., Didry, D., and Carlier, M.-F. (2010). Vinculin is a dually regulated actin filament barbed end-capping and side-binding protein. J. Biol. Chem. *285*, 23420–23432.

Lee, J., Natarajan, M., Nashine, V.C., Socolich, M., Vo, T., Russ, W.P., Benkovic, S.J., and Ranganathan, R. (2008). Surface sites for engineering allosteric control in proteins. Science *322*, 438–442.

Levchenko, I., Grant, R.A., Wah, D.A., Sauer, R.T., and Baker, T.A. (2003). Structure of a delivery protein for an AAA+ protease in complex with a peptide degradation tag. Mol. Cell *12*, 365–372.

Levskaya, A., Weiner, O.D., Lim, W.A., and Voigt, C.A. (2009). Spatiotemporal control of cell signalling using a light-switchable protein interaction. Nature *461*, 997–1001.

Lockless, S.W., and Ranganathan, R. (1999). Evolutionarily conserved pathways of energetic connectivity in protein families. Science *286*, 295–299.

Möglich, A., and Moffat, K. (2010). Engineered photoreceptors as novel optogenetic tools. Photochem. Photobiol. Sci. *9*, 1286–1300.

Nguyen, A., Rothman, D.M., Stehn, J., Imperiali, B., and Yaffe, M.B. (2004). Caged phosphopeptides reveal a temporal role for 14-3-3 in G1 arrest and S-phase checkpoint function. Nat. Biotechnol. *22*, 993–1000.

Nhieu, G.T., and Izard, T. (2007). Vinculin binding in its closed conformation by a helix addition mechanism. EMBO J. *26*, 4588–4596.

Nikolovska-Coleska, Z., Wang, R., Fang, X., Pan, H., Tomita, Y., Li, P., Roller, P.P., Krajewski, K., Saito, N.G., Stuckey, J.A., and Wang, S. (2004). Development and optimization of a binding assay for the XIAP BIR3 domain using fluorescence polarization. Anal. Biochem. *332*, 261–273.

Salomon, M., Christie, J.M., Knieb, E., Lempert, U., and Briggs, W.R. (2000). Photochemical and mutational analysis of the FMN-binding domains of the plant blue light receptor, phototropin. Biochemistry *39*, 9401–9410.

Saunders, R.M., Holt, M.R., Jennings, L., Sutton, D.H., Barsukov, I.L., Bobkov, A., Liddington, R.C., Adamson, E.A., Dunn, G.A., and Critchley, D.R. (2006).

Role of vinculin in regulating focal adhesion turnover. Eur. J. Cell Biol. *85*, 487–500.

Singh, N., Jabeen, T., Sharma, S., Roy, I., Gupta, M.N., Bilgrami, S., Somvanshi, R.K., Dey, S., Perbandt, M., Betzel, C., et al. (2005). Detection of native peptides as potent inhibitors of enzymes. Crystal structure of the complex formed between treated bovine alpha-chymotrypsin and an autocatalytically produced fragment, Ile-Val-Asn-Gly-Glu-Glu-Ala-Val-Pro-Gly-Ser-Trp-Pro-Trp, at 2.2 angstroms resolution. FEBS J. *272*, 562–572.

Strickland, D., Moffat, K., and Sosnick, T.R. (2008). Light-activated DNA binding in a designed allosteric protein. Proc. Natl. Acad. Sci. USA *105*, 10709–10714.

Strickland, D., Yao, X., Gawlak, G., Rosen, M.K., Gardner, K.H., and Sosnick, T.R. (2010). Rationally improving LOV domain-based photoswitches. Nat. Methods *7*, 623–626.

Swartz, T.E., Corchnoy, S.B., Christie, J.M., Lewis, J.W., Szundi, I., Briggs, W.R., and Bogomolni, R.A. (2001). The photocycle of a flavin-binding domain of the blue light photoreceptor phototropin. J. Biol. Chem. *276*, 36493–36500.

Swartz, T.E., Wenzel, P.J., Corchnoy, S.B., Briggs, W.R., and Bogomolni, R.A. (2002). Vibration spectroscopy reveals light-induced chromophore and protein structural changes in the LOV2 domain of the plant blue-light receptor phototropin 1. Biochemistry *41*, 7183–7189.

Thompson, G., Owen, D., Chalk, P.A., and Lowe, P.N. (1998). Delineation of the Cdc42/Rac-binding domain of p21-activated kinase. Biochemistry *37*, 7885–7891.

Tran Van Nhieu, G., Ben-Ze'ev, A., and Sansonetti, P.J. (1997). Modulation of bacterial entry into epithelial cells by association between vinculin and the Shigella IpaA invasin. EMBO J. *16*, 2717–2729.

Wu, Y.I., Frey, D., Lungu, O.I., Jaehrig, A., Schlichting, I., Kuhlman, B., and Hahn, K.M. (2009). A genetically encoded photoactivatable Rac controls the motility of living cells. Nature *461*, 104–108.

Yao, X., Rosen, M.K., and Gardner, K.H. (2008). Estimation of the available free energy in a LOV2-J alpha photoswitch. Nat. Chem. Biol. *4*, 491–497.

Yazawa, M., Sadaghiani, A.M., Hsueh, B., and Dolmetsch, R.E. (2009). Induction of protein-protein interactions in live cells using light. Nat. Biotechnol. *27*, 941–945.

Young, D.D., and Deiters, A. (2007). Photochemical control of biological processes. Org. Biomol. Chem. *5*, 999–1005.

Zoltowski, B.D., Vaccaro, B., and Crane, B.R. (2009). Mechanism-based tuning of a LOV domain photoreceptor. Nat. Chem. Biol. *5*, 827–834.